ResearchGate

See discussions, stats, and author profiles for this publication at: https://www.researchgate.net/publication/43438654

Origin of the deep Bering Sea nitrate deficit: Constraints from the nitrogen and oxygen isotopic composition of water column nitrate and benthic nitrate fluxes

Article *in* Global Biogeochemical Cycles · January 2005

DOI: 10.1029/2005GB002508 · Source: OAI

CITATIONS
80

READS
44

8 authors, including:

Moritz Felix Lehmann
University of Basel
115 PUBLICATIONS **4,097** CITATIONS
SEE PROFILE

Daniel M Sigman
Princeton University
291 PUBLICATIONS **21,984** CITATIONS
SEE PROFILE

Daniel McCorkle
Woods Hole Oceanographic Institution
129 PUBLICATIONS **6,731** CITATIONS
SEE PROFILE

Markus Kienast
Dalhousie University
119 PUBLICATIONS **3,912** CITATIONS
SEE PROFILE

Some of the authors of this publication are also working on these related projects:

Project
Collaborative Research: Isotopic and Compositional Investigation of the Sources and Interactions of Reactive Nitrogen in the Marine Atmosphere at Bermuda View project

Project
Determining phytoplankton community function and nitrate and ammonium assimilation using nitrogen isotopes View project

All content following this page was uploaded by Markus Kienast on 16 May 2014.

The user has requested enhancement of the downloaded file.

Origin of the deep Bering Sea nitrate deficit: Constraints from the nitrogen and oxygen isotopic composition of water column nitrate and benthic nitrate fluxes

Moritz F. Lehmann,[1,2] Daniel M. Sigman,[1] Daniel C. McCorkle,[3] Brigitte G. Brunelle,[1] Sharon Hoffmann,[3] Markus Kienast,[4] Greg Cane,[1] and Jaclyn Clement[5]

Received 11 March 2005; revised 19 June 2005; accepted 8 August 2005; published 12 October 2005.

[1] On the basis of the normalization to phosphate, a significant amount of nitrate is missing from the deep Bering Sea (BS). Benthic denitrification has been suggested previously to be the dominant cause for the BS nitrate deficit. We measured water column nitrate $^{15}N/^{14}N$ and $^{18}O/^{16}O$ as integrative tracers of microbial denitrification, together with pore water-derived benthic nitrate fluxes in the deep BS basin, in order to gain new constraints on the mechanism of fixed nitrogen loss in the BS. The lack of any nitrate isotope enrichment into the deep part of the BS supports the benthic denitrification hypothesis. On the basis of the nitrate deficit in the water column with respect to the adjacent North Pacific and a radiocarbon-derived ventilation age of ~50 years, we calculate an average deep BS (>2000 m water depth) sedimentary denitrification rate of ~230 μmol N m^{-2} d^{-1} (or 1.27 Tg N yr^{-1}), more than 3 times higher than high-end estimates of the average global sedimentary denitrification rate for the same depth interval. Pore water-derived estimates of benthic denitrification were variable, and uncertainties in estimates were large. A very high denitrification rate measured from the base of the steep northern slope of the basin suggests that the elevated average sedimentary denitrification rate of the deep Bering calculated from the nitrate deficit is driven by organic matter supply to the base of the continental slope, owing to a combination of high primary productivity in the surface waters along the shelf break and efficient down-slope sediment focusing along the steep continental slopes that characterize the BS.

Citation: Lehmann, M. F., D. M. Sigman, D. C. McCorkle, B. G. Brunelle, S. Hoffmann, M. Kienast, G. Cane, and J. Clement (2005), Origin of the deep Bering Sea nitrate deficit: Constraints from the nitrogen and oxygen isotopic composition of water column nitrate and benthic nitrate fluxes, *Global Biogeochem. Cycles*, *19*, GB4005, doi:10.1029/2005GB002508.

1. Introduction

[2] The oceanic budget of biologically available (or "fixed") nitrogen (N) is poorly understood, and our view of it is changing rapidly. One of the most recent changes involves denitrification, the microbial reduction of NO_3^- to N_2, which occurs predominantly under conditions of low $[O_2]$, both in the ocean water column and in the sediments. There has been a drastic upward revision in estimates of the rate of denitrification in marine sediments, such that this is now the largest single flux in the N budget [*Brandes and Devol*, 2002; *Codispoti et al.*, 2001; *Middelburg et al.*, 1996]. However, the new estimates for sedimentary denitrification are highly uncertain [*Deutsch et al.*, 2004]. Increased confidence in the overall rate estimates will require a better understanding of the partitioning of benthic denitrification between shallow (e.g., coastal) and deep (e.g., open ocean) sediments.

[3] Deviations in the $[NO_3^-]$-to-$[PO_4^{3-}]$ relationship from the Redfield ratios for algal assimilation and remineralization are used to study the rates and distributions of inputs to and outputs from the oceanic fixed N reservoir. If P behaves according to Redfield stoichiometry during remineralization (i.e., with no dramatic variations in preservation among the N and P in organic matter nor P retention in sediments), then N*, defined as $[NO_3^-] - 16*[PO_4^{3-}] + 2.9$ (in μmol L^{-1}) [*Deutsch et al.*, 2001], quantifies excesses and deficits in NO_3^- relative to the globally derived $[NO_3^-]$-to-$[PO_4^{3-}]$ relationship. These NO_3^- excesses and deficits indicate

[1]Department of Geosciences, Princeton University, Princeton, New Jersey, USA.
[2]Now at Geochemistry and Geodynamics Research Center (GEOTOP-UQAM-McGill), University of Quebec at Montreal, Montreal, Quebec, Canada.
[3]Woods Hole Oceanographic Institution, Woods Hole, Massachusetts, USA.
[4]Department of Oceanography, Dalhousie University, Halifax, Nova Scotia, Canada.
[5]Department of Oceanography, Naval Postgraduate School, Monterey, California, USA.

Copyright 2005 by the American Geophysical Union.
0886-6236/05/2005GB002508$12.00

regions of fixed N input (e.g., N_2 fixation) and loss (e.g., denitrification and alternative modes of N_2 production). When combined with some measure of ocean circulation, rates of these processes can be derived [*Deutsch et al.*, 2001; *Gruber and Sarmiento*, 1997]. While this use of nutrient data is extremely powerful, it has limitations. First, deviations from the Redfield [NO_3^-]-to-[PO_4^{3-}] relationship may not always be due to N inputs or outputs, arising instead from variations in the stoichiometry of nutrient uptake and remineralization. Second, N* does not in itself provide much contextual information about the fluxes it uncovers. For example, a nitrate deficit in the water column of a low-[O_2] basin is likely the result of denitrification, but the nitrate loss may have occurred either in the water column or the sediments.

[4] The reduction of nitrate associated with denitrification preferentially consumes $^{14}NO_3^-$, so its occurrence leads to a marked increase in NO_3^- $^{15}N/^{14}N$ in oceanic regions of suboxia [*Altabet et al.*, 1999; *Brandes et al.*, 1998; *Cline and Kaplan*, 1975; *Voss et al.*, 2001]. Denitrification in the ocean water column has consistently yielded estimates of 20–30‰ for the isotope effect for denitrification [*Brandes et al.*, 1998; *Cline and Kaplan*, 1975; *Liu and Kaplan*, 1989; *Sigman et al.*, 2003; *Voss et al.*, 2001], which is similar to at least some estimates from cultures [*Barford et al.*, 1999; *Mariotti et al.*, 1981]. By contrast, the "effective" (versus biological) isotope effect can be substantially reduced if denitrification is limited by the diffusive supply of nitrate to the denitrifying organism [*Bender*, 1990]. In marine sediments, nitrate is often completely consumed within the zone of denitrification, and sedimentary denitrification in a variety of environments has been shown to cause very little net isotope enrichment of oceanic NO_3^- [*Brandes and Devol*, 1997, 2002; *Lehmann et al.*, 2004; *Sigman et al.*, 2001]. This aspect of N isotope systematics provides a critical constraint on the relative importance of water column versus sedimentary denitrification on a global scale [*Brandes and Devol*, 2002] and in isolated basins [*Sigman et al.*, 2003]. This constraint is further strengthened by coupled measurement of the $^{18}O/^{16}O$ of NO_3^-, which addresses the possibility of multiple reactions with opposing effects on the N isotopes [*Lehmann et al.*, 2004; *Sigman et al.*, 2005].

[5] The Bering Sea (BS) is one of the largest marginal seas on Earth. It is characterized by high biological productivity and high nutrient regeneration rates [e.g., *Saino et al.*, 1979; *Tsunogai et al.*, 1979].[1] "Unusual" water column stoichiometric relationships (for example, with respect to the adjacent subarctic Pacific) among Si, P, and N were first observed and described more then 2 decades ago [e.g., *Broecker and Peng*, 1982; *Toggweiler*, 1983]. However, to date, biogeochemical cycling and processes controlling the distribution of nutrients within the deep BS remain incompletely understood.

[6] It has been shown earlier [*Broecker and Peng*, 1982; *Toggweiler*, 1983] and is confirmed below that, on the basis of normalization to phosphate, there is a ~3 μmol L^{-1} apparent nitrate deficit in the deep BS that does not exist in deep open North Pacific waters of the same density. Because the O_2 concentration of BS deep waters is 50–100 μmol L^{-1}, much higher than is typically expected to support active denitrification [*Codispoti et al.*, 2005], *Broecker and Peng* [1982] tentatively explained the nitrate deficit as the result of denitrification in the BS sediments. If so, this would represent the only known region of the deep ocean where benthic denitrification is proceeding at adequate rates to produce a clear N-to-P anomaly.

[7] Our goal here is to quantify the fraction of the deep nitrate deficit in the BS that is driven by sedimentary denitrification, using two different approaches. First, we use measurements of the N and O isotopic composition and concentration of water column nitrate as an integrative tracer of microbial denitrification. Second, we use direct in situ pore water nitrate and O_2 concentration measurements to estimate local net nitrate flux at the sediment-water interface, N remineralization, and total in situ benthic denitrification rates.

[8] These two approaches have very different strengths and weaknesses and thus complement one another. The pore water measurements are inherently more direct as a measure of benthic nitrate consumption, so that there is little doubt about which processes are being measured. However, they are hard to extrapolate to the basin scale because they include no mechanism (other than multiple samplings) to account for spatial or temporal heterogeneity in seafloor processes. The nitrate isotopes are inherently less direct and certain as an indicator of seafloor processes. However, deep ocean nitrate integrates over large scales of space and time. Thus, with the right complementary constraints (e.g., estimates of ventilation rate), the hydrographic approach provides a more robust measure of the basin-mean rate of nitrate loss.

2. Materials and Methods

2.1. Sample Collection and Hydrochemical Analyses

[9] Depth profiles of water samples were collected by hydrocast at stations along two connected transects in the BS during cruise HLY 02-02 aboard the USCGC *Healy* in June 2002: (1) a north-south transect between the northern BS and Bowers Ridge and (2) an east-west transect between the Bowers Ridge and the shelf-break in the southeast BS (Figure 1). An additional water column profile was taken south of the Bowers ridge in the Bowers Basin. Water column samples were collected using 12-L Niskin bottles attached to a 24-bottle rosette. Sub-samples were collected in 5% HCl- and deionized water-cleaned polyethylene bottles and were preserved by freezing.

[10] From frozen water column sample aliquots, nitrate, nitrite, and phosphate were determined onboard using standard automated colorimetric methods following WOCE/JGOFS nutrient analyses protocols as described in the JGOFS Report 19 [*Scientific Committee on Oceanographic Research* (*SCOR*), 1996]. Ammonium concentrations were measured onboard using a phenol-hypochlorite protocol similar to that described by *Whitledge et al.* [1981]; ammonium in the deep BS was always close to detection

[1] Auxiliary material is available at ftp://ftp.agu.org/apend/gb/2005GB002508.

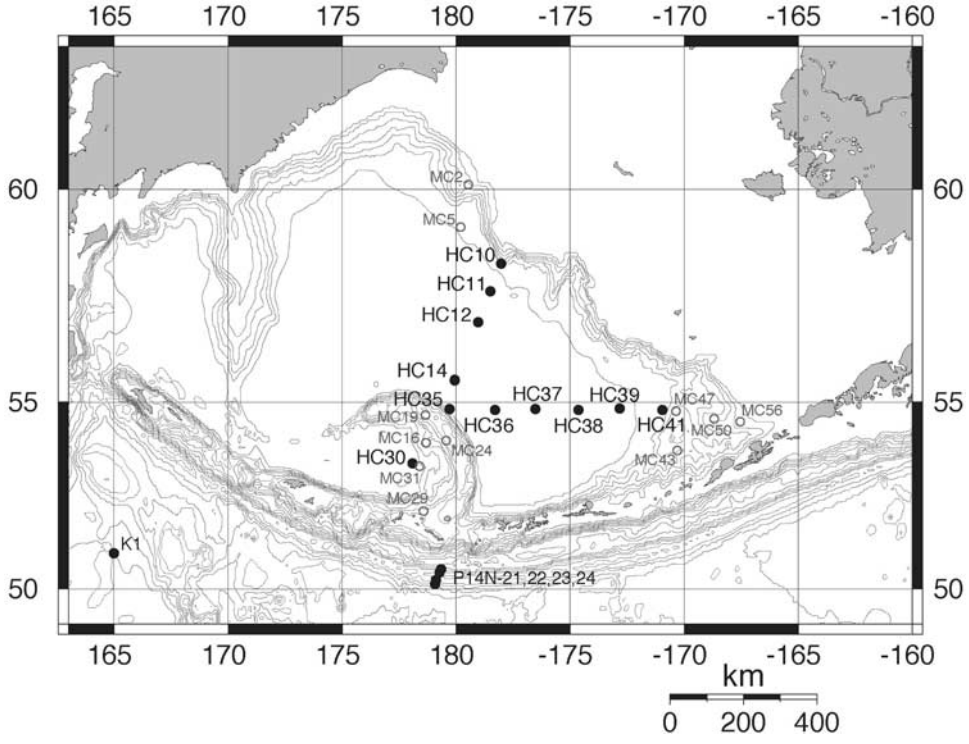

Figure 1. Map showing the Bering Sea hydrocast (HC) and multicore (MC) sampling locations for cruise WAGB 20 in the summer 2002 (USCGC *Healy*). Also indicated are four hydrocast sampling stations outside the Bering basin from WOCE cruise P14N in 1996, and the sampling location K1 for nitrate isotope profiles taken from M. Kienast et al. (manuscript in preparation, 2005). Bathymetric contours are shown at 500-m intervals.

limits. The concentration of dissolved O_2 was determined by Winkler titration.

[11] Multicores were collected from three different regions: (1) the northern BS slope, (2) the Bowers Ridge region and (3) the southeast BS slope (Figure 1). The coring sites cover depths from 700 m to 3500 m. Subcores were processed immediately after corer recovery at near-in situ temperatures (4°C) in a shipboard environmental chamber. Pore water samples were collected from one subcore using shipboard whole core squeezing (WCS) [*Martin et al.*, 1991] and from another subcore using sediment sectioning and centrifugation followed by 0.45 μM membrane filtration. The WCS was intended to provide good depth resolution near the sediment-water interface, while the core sectioning provided deeper pore water samples. All samples were frozen immediately and were stored frozen. A third subcore was profiled immediately after recovery with a manual O_2 minielectrode profiling system to establish core top O_2 gradients. O_2 content of overlying water samples was determined by small-volume Winkler titration. Porosity for the calculation of effective solute diffusivities was determined for the top 3 cm of each core by weighing samples of known volume before and after drying in the oven. Nitrate + nitrite (hereinafter referred to as "nitrate") concentrations from frozen pore water samples were determined in Princeton by reduction to nitric oxide (NO) in a heated solution of acidic V(III) and chemiluminescent detection of the NO [*Braman and Hendrix*, 1989].

2.2. Benthic Flux Calculations

[12] Net nitrate fluxes at the sediment water interface were calculated from high-resolution nitrate profiles using Fick's first law, $F = D_{sed}\Delta C/\Delta z$, where D_{sed} is the diffusion coefficient for nitrate corrected for temperature and sediment porosity [*Boudreau*, 1997], and $\Delta C/\Delta z$ is the nitrate concentration gradient with depth z in the sediment. $\Delta C/\Delta z$ is calculated from the linear portion of the nitrate concentration profile just below the sediment-water interface. Nitrate gradients were also calculated from nitrate profiles generated by the analysis of water from centrifuged core samples, and, in general, we found good agreement between the two methods. O_2 fluxes were calculated from exponential-fit gradients at the sediment-water interface.

2.3. Nitrate Isotope Analyses

[13] Natural abundance level N and O isotope analyses of nitrate were performed using the denitrifier method of [*Casciotti et al.*, 2002; *Sigman et al.*, 2001]. Briefly, sample nitrate is converted to nitrous oxide (N_2O) by denitrifying bacteria that lack N_2O reductase activity (*Pseudomonas chlororaphis*, ATCC 43928 or *Pseudomonas chlororaphis*

ATCC 13985 (formerly *Pseudomonas aureofaciens*, referred to below as such). N_2O is stripped from the sample vial using helium as carrier gas, purified, and analyzed for its N and O isotopic composition. The determination of the $^{18}O/^{16}O$ of nitrate requires the correction for fractionation during O atom removal and exchange with O atoms from water during the reduction of nitrate to nitrous oxide [*Casciotti et al.*, 2002]. O isotope exchange was always <3% (for *P. aureofaciens*). Blank contribution was generally lower than 0.3 nmol (as compared to 20 nmol of sample N). The use of *P. aureofaciens* allows for the simultaneous analysis of nitrate $^{15}N/^{14}N$ and $^{18}O/^{16}O$ ratios, whereas *P. chlororaphis* is used for N isotope analysis only [*Casciotti et al.*, 2002]. There was good agreement between $^{15}N/^{14}N$ measurements using *P. aureofaciens* and those using *P. chlororaphis*, and N isotope data reported here were derived using either bacterial strain. N and O isotope ratios are reported in the conventional δ-notation with respect to atmospheric N_2 and deep Pacific nitrate (see below), respectively:

$$\delta_{\text{sample}} = \left(\frac{R_{\text{sample}}}{R_{\text{standard}}} - 1\right) \times 1000, \quad (1)$$

where R represents the $^{15}N/^{14}N$ or $^{18}O/^{16}O$ ratio, respectively. On the basis of replicate measurements of laboratory standards and samples, the analytical precision for $\delta^{15}N$ and $\delta^{18}O$ was generally better than ±0.2‰ and ±0.3‰ (1 SD), respectively.

[14] The denitrifier method can only measure the O isotope ratio differences among nitrate samples and standards. Here isotope values were calibrated using IAEA-N3, an international KNO_3^- reference material with a reported $\delta^{18}O$ of +22.7 to +25.6‰ (relative to V-SMOW) [*Bohlke et al.*, 2003; *Lehmann et al.*, 2003; *Revesz et al.*, 1997; *Silva et al.*, 2000], and an assigned $\delta^{15}N$ of +4.7‰ relative to atmospheric N_2 gas [*Gonfiantini et al.*, 1995]. We adopt here a $\delta^{18}O$ for IAEA-N3 of +22.7‰ (V-SMOW), for consistency with our previous manuscripts. If the most recent assignment for IAEA-N3 of 25.6‰ [*Bohlke et al.*, 2003] is proven correct, then our $\delta^{18}O$ values reported relative to V-SMOW will need to be shifted upward by ~2.9‰. However, this is not of fundamental concern for the present study.

3. Results

3.1. Nutrient and Oxygen Concentrations in the Water Column

[15] The distributions of nitrate and phosphate are relatively invariant across the open Bering Sea, with highest concentrations of nitrate and phosphate (45–46 μmol L^{-1} and 3.2–3.3 μmol L^{-1}, respectively) at ~500 m and an upward decrease to roughly half these values in the surface (Figure 2). The lack of large spatial gradients in the open basin of the Bering stands in stark contrast to a rapid decrease in nutrients as one moves from the open basin to the shelf [e.g., *Tanaka et al.*, 2004]. The nutrient concentrations decrease from 500 m into the deeper basin, more for nitrate than for phosphate, as described below.

[16] As described above, N* can be used to detect deviations in the ratio of $[NO_3^-]$ to $[PO_4^{3-}]$ from those expected from the internal N cycle (N assimilation and remineralization/nitrification), given Redfield stoichiometry [*Gruber and Sarmiento*, 1997]. Generally, negative N* in the ocean interior indicates a net loss of nitrate, most likely due to denitrification. Consistent with earlier work, we measured a very low N* in the deep BS, −5 to −6 μM (Figure 2). The low N* of the deep BS is not observed in the adjacent subarctic Pacific (SAP) (Figure 2c). The SAP deep water represents the main source of BS deep water, advected into the Kamchatka Basin through the Kamchatka Strait and then into the main Bering basin [*Coachman et al.*, 1999; *Reed et al.*, 1993; *Toggweiler*, 1983]. The N* of SAP subsurface and deep water ranges between −3 and −1 μmol L^{-1}, on average 3 μmol L^{-1} higher than in the deep BS and increasing toward the bottom. Comparison of the nutrient data between the BS and SAP (Figures 2a and 2b) indicates that the nitrate distributions are very similar whereas the phosphate distributions are not; phosphate concentrations are higher in the deep BS than in the SAP.

[17] The discrepancy between the BS and SAP N/P ratios is reduced in the deepest 200 m of the BS water column, as indicated by a marked break in N* toward less negative values. This change is driven by a decrease in $[PO_4^{3-}]$ and is associated with higher $[O_2]$. These geochemical properties seem to be associated with a benthic layer recognized by previous investigators and most recently explained as the result of inputs of SAP deep water that have spilled into the BS through the Kamchatka Strait to fill the bottom of the basin [*Coachman et al.*, 1999].

[18] The N* in the surface waters of the BS is even lower than that observed in the deep basin, with values as low as −7 μmol L^{-1}. Similarly low $[NO_3^-]/[PO_4^{3-}]$ has been reported from the southeastern BS shelf by *Tanaka et al.* [2004], who interpreted this as the result of benthic denitrification on the extensive BS shelf, an explanation that seems sensible in light of previous benthic chamber results [e.g., *Devol et al.*, 1997]. Hence high denitrification rates on the Bering shelf [*Devol et al.*, 1997; *Koike and Hattori*, 1979; *Tanaka et al.*, 2004] and strong lateral mixing in the upper layer of the water column best explains the basin wide shallow N* minimum. CFC's have been reported from the deep layer in the BS [*Warner and Roden*, 1995], raising the possibility that this deep layer is also affected by deep water formation on the BS shelf. The role of the BS shelf in the amplitude and structure of the deep BS N* is addressed below.

[19] The O_2 concentration profiles exhibit a typical $[O_2]$ minimum between 500 and 1000 m water depth (Figure 2d). Importantly, the lowest O_2 concentrations encountered were ≥15 μmol L^{-1}. Thus no portion of the O_2 minimum zone (OMZ) was found to be adequately low in $[O_2]$ to encourage water column denitrification (~5 μmol L^{-1}) [*Codispoti et al.*, 2005].

3.2. Nitrate Isotopes in the Water Column

[20] Like $[NO_3^-]$, the distribution of nitrate $\delta^{15}N$ and $\delta^{18}O$ varies little across the open BS (Figure 3). All isotope profiles show enrichment in ^{15}N and ^{18}O in surface water

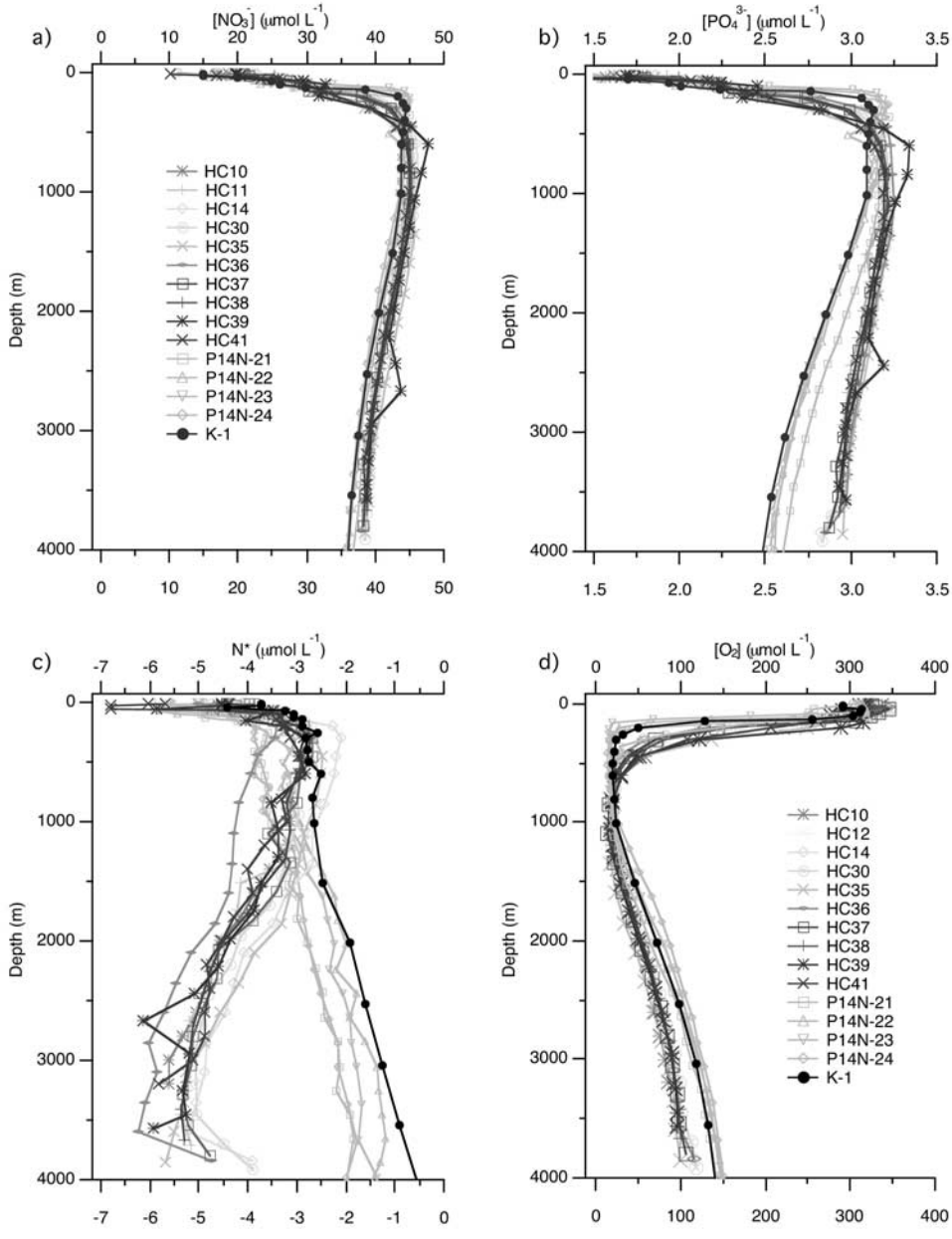

Figure 2. Water column profiles of (a) $[NO_3^-]$, (b) $[PO_4^{3-}]$, (c) N*, and (d) $[O_2]$ for Bering Sea stations (HC) and Stations from the subarctic Pacific (P14N and K1). Nutrient data are not available for BS station HC12, and $[O_2]$ data are not available for BS station HC11. Note the stoichiometric differences between the BS and the SAP. See color version of this figure at back of this issue.

nitrate, in association with reduced $[NO_3^-]$. The enrichment presumably results from isotope fractionation during algal NO_3^- assimilation, with preferential consumption of $^{14}N^{16}O_3$ relative to both ^{15}N- and ^{18}O- bearing nitrate, as has been observed previously in the laboratory [e.g., *Granger et al.*, 2004; *Wada and Hattori*, 1978; *Waser et al.*, 1998] and in field studies [e.g., *Altabet*, 2001; *Altabet and Francois*, 1994; *Casciotti et al.*, 2002].

[21] The isotopic composition of subsurface and deep-water nitrate varies little with water depth. In the depth-binned average nitrate isotope profiles (Figures 3c and 3d), very subtle N and O isotope ratio maxima in association with the $[O_2]$ minimum can be observed. Below 1500 m, the $\delta^{15}N$ decreases slightly by about 0.35‰ to reach 5.3‰ in the bottom water, while the nitrate $\delta^{18}O$ remains more or less constant at around $+0.2 \pm 0.2$‰.

[22] If the observed nitrate deficit (i.e., low N* values) in the deep BS were caused by denitrification in the water column, we would expect N and O isotope enrichment due to isotope discrimination (Figure 3c and 3d), as

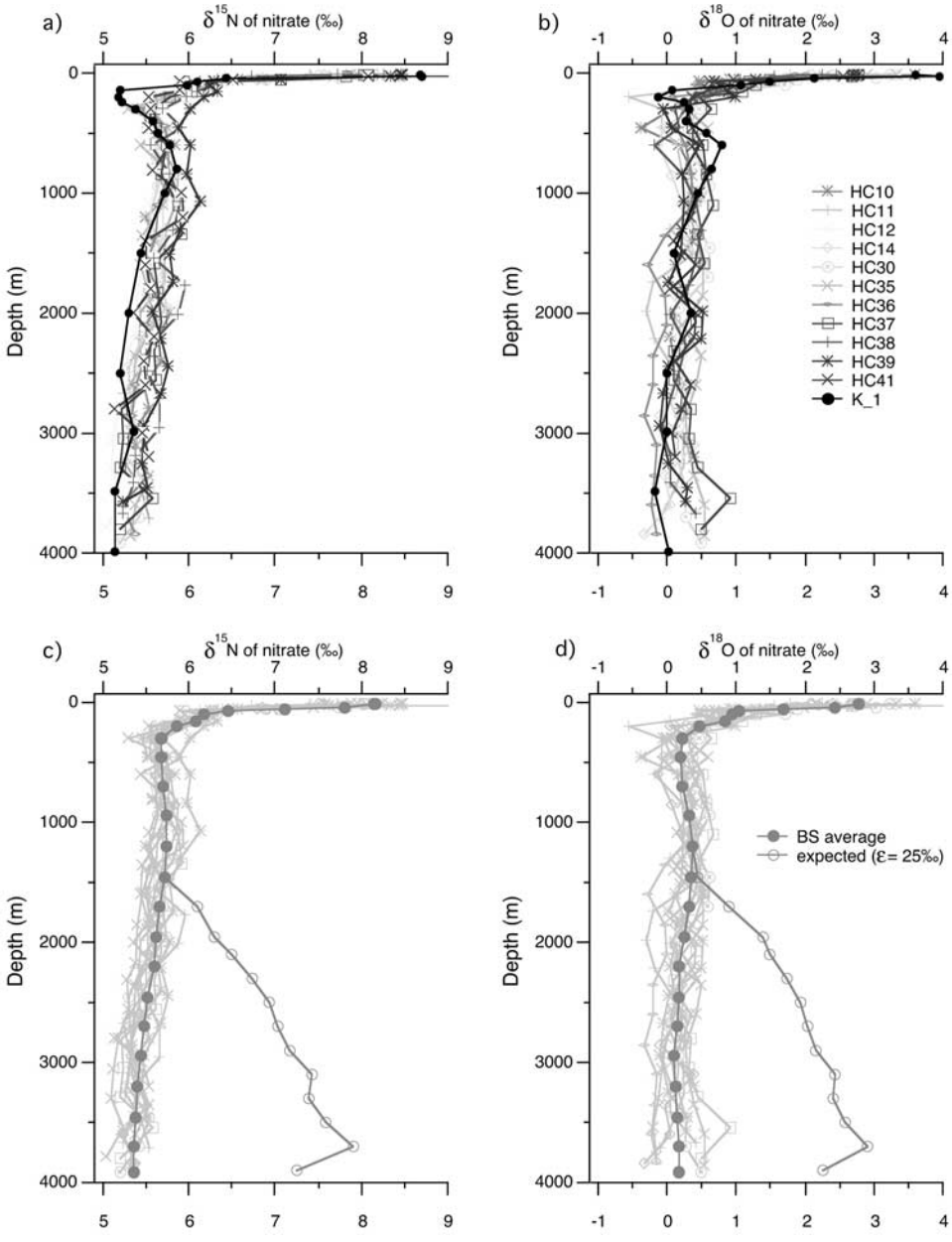

Figure 3. Water column profiles of (a) nitrate $\delta^{15}N$ and (b) nitrate $\delta^{18}O$ for Bering Sea stations (HC) and Station K1 from the subarctic Pacific (K1 nitrate isotope data are taken from M. Kienast et al. (manuscript in preparation, 2005)). (c, d) Solid circles represent depth-binned average nitrate isotope values for all the BS hydrocasts superimposed on the profiles shown in Figures 3a and 3b. Expected N and O isotope ratios (open symbols in Figures 3c and 3d) are based on an assumed isotope effects $\varepsilon_{15} = \varepsilon_{18} = 25‰$ for denitrification and the observed nitrate deficit below 1500 m water depth, assuming a steady state balance between gross supply of SAP nitrate, partial nitrate consumption, and export by circulation of the remaining nitrate. See color version of this figure at back of this issue.

has been observed in previous studies [*Brandes et al.*, 1998; *Sigman et al.*, 2003; *Voss et al.*, 2001]. These field studies have suggested an isotope effect for denitrification of 20–30‰, which generally fits with culture study assessments of the organism-level isotope effect [e.g., *Barford et al.*, 1999]. Assuming an isotope effect of ~25‰, the nitrate $\delta^{15}N$ and $\delta^{18}O$ at 3000 m would be ~1.6‰ higher than observed at the N* maximum at ~750 m, assuming a steady state balance between gross supply of SAP nitrate, partial nitrate consumption, and

export by circulation of the remaining nitrate (i.e., the ''steady state'' or ''open system model'') (Figure 3). However, the large nitrate deficit found in the BS is not accompanied by a discernible N or O isotope enrichment. The lack of isotopic enrichment associated with low N* in the deep basin leaves two alternatives for the cause of the low N* of the deep BS basin. First, there is a process consuming nitrate from the deep BS that expresses no isotopic discrimination, such as has been observed for sedimentary denitrification. Second, the low N* of BS deep waters is driven not by nitrate consumption, but rather by phosphate addition.

3.3. Pore Water Measurements

[23] Pore water O_2 and nitrate concentration measurements in the multicores from pelagic BS sediments (Figure 4) indicate that, generally by 1–4 cm below the sediment-water interface, the sediments are suboxic and nitrate is being consumed. Typically by 5 cm depth, $[NO_3^-]$ has dropped below the detection limit. At most of the locations, nitrate concentration decreases continuously from the sediment-water interface into the sediments. In two cores retrieved from the deeper Bowers Basin, MC29 and MC31, O_2 penetrated significantly deeper into the sediments, and a pore water nitrate maximum was observed just below the sediment-water interface, indicating that, at those sites, nitrate production from nitrification exceeded nitrate consumption by denitrification. The nitrate and O_2 gradients at the sediment-water interface can be used to calculate nitrate and O_2 fluxes into (or out of) the sediments and, in turn, to estimate sedimentary denitrification rates.

4. Interpretation

4.1. Low N* in the Deep Bering Sea: Nitrate Loss or Excess Phosphate Addition?

[24] As described above, our isotope data beg the question of whether the low N* in the deep BS is due to the addition of phosphate rather than removal of nitrate. More efficient regeneration of P relative to C or N appears to occur in suboxic sediments [*Ingall and Jahnke*, 1994]. However, while this redox effect may be very important for the amount of P burial on geological timescales, it does not provide a mechanism for producing excess P in environments where only a minor fraction of the total accumulated carbon is preserved. Nevertheless, such logic cannot rule out some other unusual source of phosphate to the deep BS.

[25] The strongest evidence for nitrate removal and against an exotic P input term comes from the dissolved O_2 data. Deep BS waters at ~3400 m water depth have ~38 μmol L^{-1} O_2 less than the deep SAP (Figure 2d). Assuming a molar ratio of 138:1 for O_2 consumption versus P release during organic matter remineralization in the abyss [*Froelich et al.*, 1979], one would predict ~0.28 μmol L^{-1} additional PO_4^{3-} in the deep BS, which is close to the observed BS-SAP difference of 0.36 μM at 3400 m. Extending this calculation, one would expect 4.4 μM additional NO_3^-, which is clearly greater than the amount observed, supporting the interpretation of NO_3^- loss from the deep BS waters. Moreover, calculating the nitrate deficit from O_2 concentrations is conservative, since suboxic and anoxic organic matter degradation can replace aerobic respiration and remineralize P without O_2 loss. We conclude that most of the differences in the concentrations of phosphate and O_2 between the deep BS and SAP can be explained by ''normal'' organic matter remineralization while the distribution of nitrate cannot.

4.2. Origin of the Nitrate Deficit in the Deep Bering Sea

[26] The nutrient data indicate that nitrate is missing from the deep BS, owing to a sink of N in the deep BS or in the ocean regions that fill the deep BS basin. The isotope data provide an additional constraint, indicating that the nitrate loss occurs without measurable discrimination of the N or O isotopes. In previous studies of N loss where only the N isotopes of nitrate were measured, ambiguities remained when a lack of ^{15}N enrichment was noted, as it was difficult to rule out the possibility of an ^{15}N-enriching process such as pelagic denitrification being countered by the production of ^{15}N-depleted nitrate. The latter could result from the remineralization of organic matter with a $\delta^{15}N$ lower than that of bottom water or from the interaction of the fractionating oxidation of ammonium and/or nitrite with recently recognized mechanisms of fixed N loss other than denitrification [e.g., *Kuypers et al.*, 2003]. With the additional capability to measure the O isotopes in nitrate, these possibilities can be addressed [*Lehmann et al.*, 2003, 2004; *Sigman et al.*, 2003]. For example, if the deep nitrate deficit were generated by denitrification with an isotope effect of 25‰ but the resultant ^{15}N enrichment were completely countered by an input of low $\delta^{15}N$ N, the $\delta^{18}O$ would still be elevated by ~3.6‰, which is clearly not observed. Hence the lack of heavy isotope enrichment in the deep BS for both the N and O isotopes of nitrate confirm that the nitrate consuming process lacks an effective isotope discrimination.

[27] Isotope studies have clearly shown the importance of transport limitation in causing severe underexpression of isotope effects at the organism level of denitrification. This effect was first noted in coastal sediments by *Brandes and Devol* [1997], has been replicated in several shallow marine environments [*Brandes and Devol*, 2002; *Lehmann et al.*, 2004], and is the most obvious explanation for the lack of isotope enrichment associated with the deep BS nitrate deficit. However, several questions must be addressed. First, is it clear that denitrification in the deep BS sediments would proceed without fractionation? If not, we would need to turn to some other source for the nitrate deficit, such as import of the nitrate deficit from BS shelf through deep water formation. Second, are there alternative causes for a complete lack of isotope effect expression during denitrification, such as denitrification in sinking particles?

4.2.1. Isotope Effect Expression in Sedimentary Denitrification

[28] Sedimentary denitrification in the Puget Sound [*Brandes and Devol*, 1997] and the Santa Monica Bay [*Lehmann et al.*, 2004] has been shown to occur with N

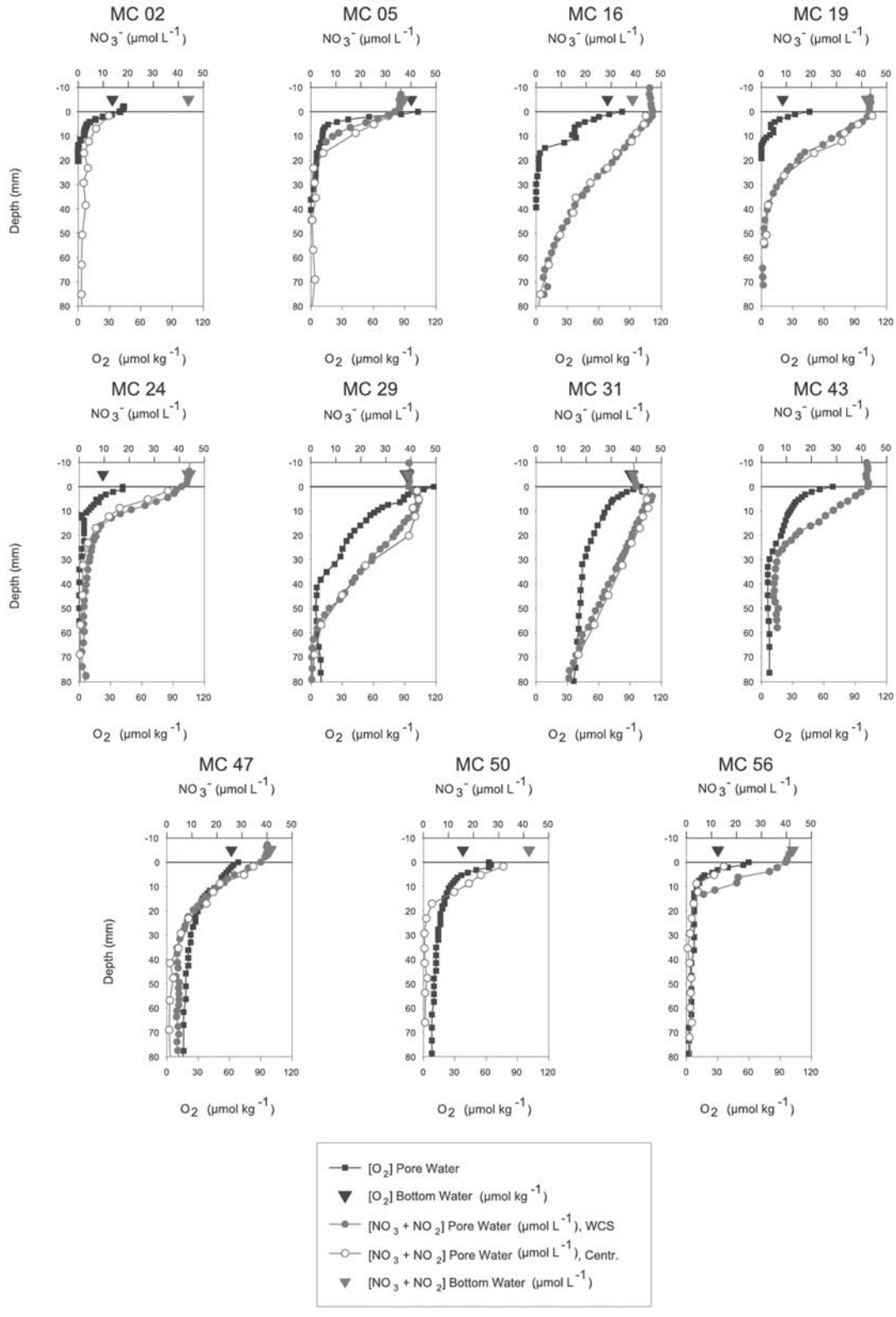

Figure 4. Pore water profiles ($[NO_3^- + NO_2^-]$ and $[O_2]$) for multicores from the Bering Basin. O_2 profiles were generated using a shipboard minielectrode profiler. Deviations between the Winkler-derived $[O_2]$ in the bottom water (sample taken from Niskin bottle) (open triangle) and electrode-derived $[O_2]$ at the sediment water interface are due to atmospheric contamination during shipboard profiling. Low non-zero $[O_2]$ values deep in some profiles may reflect bottom water leakage along the electrode, rather than real pore water $[O_2]$. See color version of this figure at back of this issue.

and O isotope effects of ~0–1‰, owing to limitation in the diffusive supply of nitrate from overlying waters into the sediments. Are these observations generally valid for all sedimentary environments, especially for pelagic sediments with much lower denitrification rates?

[29] Shelf sediments from the Santa Monica Bay are highly irrigated, such that bottom waters might be expected to be put in close contact with the zones of denitrification, allowing for ^{15}N and ^{18}O-enriched nitrate to escape into the chamber water. Yet no significant ^{15}N or ^{18}O enrichment was noted in the benthic chamber nitrate as nitrate consumption proceeded [*Lehmann et al.*, 2004]. Likewise, studies of deeper sedimentary environments are consistent with no isotopic expression for sedimentary denitrification. In pore water profiles from the Carolina slope in the western N-Atlantic [*Sigman et al.*, 2001] and from the BS itself [*Lehmann et al.*, 2002], large downward increases in nitrate $\delta^{15}N$ (and $\delta^{18}O$) are observed coincident with the decrease in nitrate concentration, owing to isotopic fractionation during denitrification. However, isotope fractionation seems to be poorly expressed at the scale of sediment-water nitrate exchange in these environments as well. In a subsequent manuscript, we will address this question more quantitatively in the context of a large set of nitrate isotope measurements in deep BS pore water profiles.

4.2.2. Import of the Nitrate Deficit From the BS Shelf

[30] It seems unlikely that the deep water nitrate deficit originates from benthic denitrification occurring on the BS shelf. The N* on the shelf (−6 to −7 μmol L^{-1}; data not shown) is not much lower than that observed in the deep BS (~−6 μmol L^{-1}) such that deep water formation would need to account for nearly the entire water volume below 2000 m. The CFC levels observed in deep BS are not anywhere near so abundant as to allow for such a wholesale transfer of water from the shelf [*Warner and Roden*, 1995], and the physical conditions of the shelf are clearly not capable of maintaining such a rate of deep water formation [*Coachman et al.*, 1999; *Warner and Roden*, 1995]. This possibility is also inconsistent with the $\Delta^{14}C$ data generated from our hydrocast samples (D. McCorkle and A. McNichol, unpublished data, 2004), and the shape of the N* profiles argue against even a modest shelf source. If low-N* water from the shelf or the open BS surface waters was spilling into the abyss, we would expect to observe a basal N* minimum. Yet, the N* in the abyssal BS increases toward the ocean floor in the deepest samples (Figure 2d). While the increase in N* as one enters this bottom layer is in the opposite sense to what one would expect from the input of BS surface waters, it is completely consistent with inputs of deep SAP water.

4.2.3. Other Mechanisms for Denitrification Without Isotope Discrimination

[31] While the observed O_2 levels in the BS argue against water column denitrification, there is some uncertainty about the universal inhibition of denitrification by O_2 [*Lloyd*, 1993; *Yoshinari and Koike*, 1994]. In any case, the lack of ^{15}N and ^{18}O enrichment in deep BS nitrate rules out this process acting alone. However, respiration in sinking organic particles may reduce O_2 adequately to encourage denitrification. Suboxic biogeochemical signatures have been observed in particle-rich, aerobic waters [*Alldredge and Cohen*, 1987; *Wolgast et al.*, 1998]. It is reasonable to imagine that suboxic conditions can occur in settling or suspended aggregates, providing important microenvironments for denitrification in waters already relatively low in O_2, as are the subsurface waters of the BS. It is not immediately clear to what degree particle-associated denitrification would express the inherent isotope effect of this process, and it is worth considering whether it represents a viable alternative for the N* minimum in the deep BS.

[32] Experiments with field and laboratory aggregates reveal that, in large (>0.5–10 mm diameter) aggregates in which diffusion dominates, the interior can become suboxic only when the ambient water has an $[O_2]$ of 25 μmol L^{-1} or less [*Ploug*, 2001]. While $[O_2]$ reaches as low as 15 μmol L^{-1} at 500 to 1250 m in the BS, $[O_2]$ is between 50 and 115 μmol L^{-1} below 2000 m. Also, in large aggregates, molecular diffusion is not the sole process of solute transfer. Fluid velocities of up to 200 μm s^{-1} in large sinking aggregates [*Logan and Alldredge*, 1989; *Ploug et al.*, 2002] make oxidant limitation even more unlikely. Thus it seems unlikely that sinking particles in the deep BS are able to reach suboxia. Moreover, given the lower $[O_2]$ of the shallower water column and the expectation for a decrease in sinking particle abundance with depth, it is hard to explain why a deep nitrate deficit would develop without a similar deficit in the upper water column, where particle flux is greater and $[O_2]$ is lower.

[33] For particle-associated denitrification to explain the deep BS nitrate deficit, not only must this process occur, it must also do so without isotope fractionation. One might imagine that some sinking particles are adequately large, reactive and slowly sinking to host denitrification. Adopting the "microsite model" of *Brandes and Devol* [1995, 1997] for water column particles, it may seem plausible that the diffusive supply of nitrate into the particle might limit the denitrification rate, such that nitrate consumption occurs without any expression of the biological isotope effect of denitrification. As described above, simply the development of suboxia in large particles is difficult, let alone the complete consumption of nitrate in waters with ≥35 μmol L^{-1} nitrate. Nevertheless, even if such complete nitrate consumption occurred in some particles, any imaginable size distribution for sinking particles would rule out complete nitrate consumption in all of them, so that there would be significant isotope fractionation with this process.

4.3. Deep BS Sedimentary Denitrification Rates

[34] Following the arguments above, sedimentary denitrification in the deep BS emerges as the principal cause for the deep nitrate deficit in the basin. Here we use the N*-derived nitrate deficit (relative to the open SAP) to derive rate estimates for fixed N loss. We then turn to the pore water measurements to understand the seafloor properties that determine these rates. It is important to note that, strictly speaking, the term denitrification we use here should be termed "free-N production", including possible alternate pathways for converting fixed N to N_2 (such as anammox). Our approach allows us only to estimate total fixed N loss

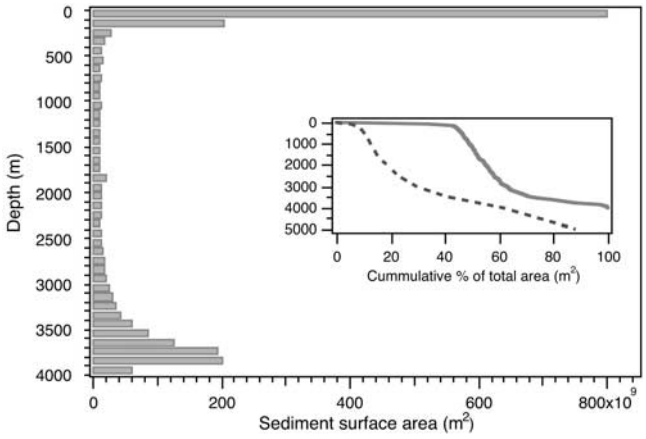

Figure 5. Bottom sediment area in the BS as function of depth (100-m intervals). The largest sediment area in the deep BS is found between ~3200 and ~3900 m water depth. Hypsographic curves for the BS (solid line) and for the global ocean (dashed line) are shown in the graph inset. A comparatively small contribution of sediments between 200 and 3000 m water depth to the total surface sediment area in the BS indicates that the slopes in the BS are relatively steep when compared to the global average continental slope. The bathymetric data for the BS are part of the ETOPO2 2-minute database and were taken from the Geographic Information Network of Alaska (GINA) of the University of Alaska (http://www.gina.alaska.edu/page.xml?group=data&page=griddata).

rates as N_2, but we do not know a priori whether denitrification in the strict sense (including coupled nitrification-denitrification) is indeed the only process that leads to the loss of N_2 from the sediments.

4.3.1. Rates Derived From the Deep Nitrate Deficit

[35] *Coachman et al.* [1999] suggested that water exchange with the SAP occurs at low rates, resulting in hydraulic residence times of approximately 300 years for the deep BS. *Tsunogai et al.* [1979] calculated an even higher residence time of 350–400 years. *Toggweiler* [1983] calculated a significantly lower residence time of 150 years. Radiocarbon analyses of water samples collected during the Healy 02-02 cruise (D. McCorkle and A. McNichol, unpublished data, 2004) revealed essentially no change in $\Delta^{14}C$ between the SAP and the deep BS along isopycnals. After correction for respiration and dissolution of the high-^{14}C organic C and $CaCO_3$ export, the ^{14}C data suggest a residence time for deep BS waters of 50 ± 50 years, somewhat shorter than Toggweiler's estimates.

[36] Using a simple one-box model with a steady input of North Pacific water, a deep BS ventilation age of 50 years, and the hypsometry of the BS basin (Figure 5), and assuming steady state, we calculate the denitrification rate per m^2 sediment area required to generate the observed deep water nitrate deficit at different depth intervals (Table 1, Figure 6). Our assumption of a constant basin residence time as a function of depth for deep BS waters is based on the observation that the BS-SAP corrected $\Delta^{14}C$ difference does not change significantly with depth in the bottom 2000 m. Average sedimentary denitrification rates for depth increments of 200 m below 2000 m water depth range between 10 and 940 μmol N m^{-2} d^{-1} (Table 1), with the lowest rates in the deepest portion of the basin (Figure 6). The decrease in area-normalized denitrification rate with depth in the lower 2000 m is qualitatively consistent with the expected downward decrease in organic carbon rain rate and with the downward increase in bottom water [O_2] [*Middelburg et al.*, 1996]. However, the model simplifies the real situation as it ignores vertical mixing and advection.

[37] In particular, as mentioned above, our data and previous results indicate a bottom layer up to 200 m thick that differs from the overlying waters in potential temperature, salinity, dissolved silicate, dissolved O_2, and N* [*Coachman et al.*, 1999; *Toggweiler*, 1983]. The characteristics of this bottom layer relative to the overlying water (colder, saltier, higher in O_2, lower in silicate, and higher in N*) indicate that it is the result of inflow from the SAP through the Kamchatka Strait [*Coachman et al.*, 1999; *Toggweiler*, 1983]. Given this evidence for water mass renewal, it is possible that the downward decrease in

Table 1. Ratio of Water Volume to Bottom Sediment Area, Observed Nitrate Deficit, and Calculated Integrative Sedimentary Denitrification Rates as a Function of Water Depth in the BS[a]

Depth segment	Water Volume/Sediment Area, m	Nitrate Deficit (Observed), μmol L^{-1}	Denitrification Rate (Modeled), μmol d^{-1} m^{-2}	Annual N Loss (Modeled), 10^{10} g N yr^{-1}
2000–2200 m	6617	2.11	726	11.9
2200–2400 m	7102	2.33	880	13.0
2400–2600 m	6843	2.67	937	14.0
2600–2800 m	5273	2.88	769	14.4
2800–3000 m	4482	3.11	708	15.0
3000–3200 m	2929	3.48	530	16.2
3200–3400 m	1478	3.60	270	15.1
3400–3600 m	926	3.63	180	13.8
3600–3800 m	290	3.70	65	10.8
3800–4000 m	72	2.80	11	1.5
2000–4000 m	**1468**	**2.96**	**230**	**127**

[a]Nitrate deficits are derived from the average difference in N* between the BS stations and SAP stations P14N-21 to 24. Using a one-box model, denitrification rates were estimated for each depth interval, assuming steady state conditions, based on the observed nitrate deficit at given depth with respect to the SAP, and water flowing in from the SAP according to a residence time of 50 years.

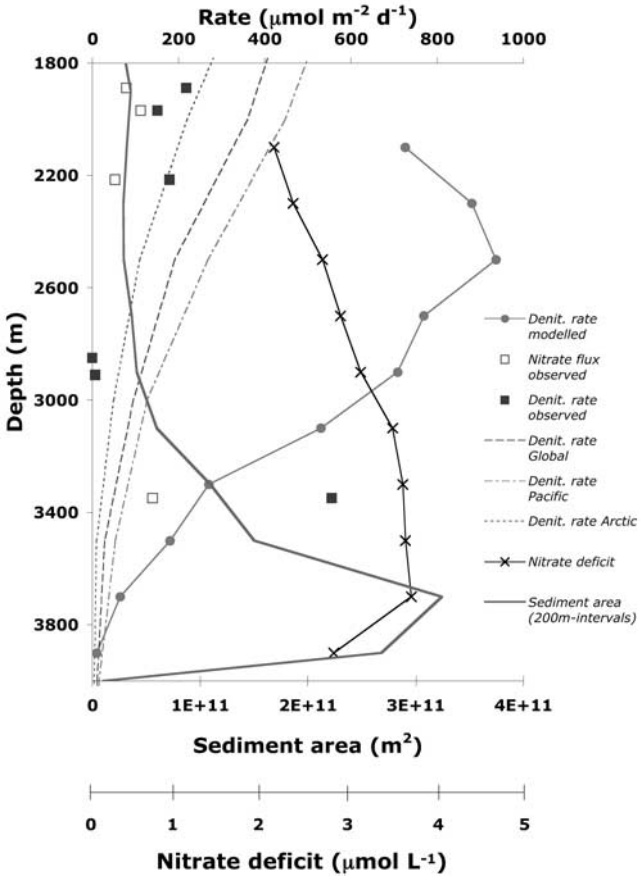

Figure 6. Compilation of directly determined nitrate fluxes and sedimentary denitrification rates (below 1900 m), and indirectly determined mean sedimentary denitrification rates based on the distribution of N*, compared to estimated sedimentary denitrification rates as a function of depth for the global ocean, the Pacific Ocean, and the Arctic Ocean from *Middelburg et al.* [1996]. Also plotted are the seafloor sediment area for given water depths (200-m intervals), and the apparent nitrate deficit calculated from the N* difference between the BS and the SAP. Apparent nitrate fluxes out of the sediments of MC29 and MC31 are not shown. See color version of this figure at back of this issue.

estimated area-normalized denitrification rate is at least partially driven by renewal of the deep BS from the bottom, with upward advection in the interior.

[38] Focusing now on the total (rather than area-normalized) rates, Table 1 shows the total annual loss of fixed N at each depth interval, with most N loss between 3000 m and 3400 m water depth. This is presumably the result of the basin bathymetry, with much of the seafloor area associated with the basin floor (Figure 6). It is tempting to argue that the increase in N* toward the bottom of the basin is due to the reduced area of seafloor at the greatest depths (Figure 6). However, these deepest waters also have the highest ratio of sediment area to water column volume, so that, for a given areal rate of sediment denitrification, N* should be more negative near the bottom, not less negative. As described above, the higher N* of the bottom layer is consistent with the inflow of high-N* water from the deep SAP, so we could turn to this as the explanation for the N* inversion near the bottom. Alternatively, it could be due to less organic matter supply to the deepest basin seafloor than to the base of the slopes, which are at ~3300–3500 m (Figure 5). In any case, the consistency between a relatively low area-normalized denitrification rate and the deep nitrate deficit indicate that the unique bathymetry of the BS, with steep slopes and a flat, extensive basin bottom (Figure 5) is in itself an important cause of the low N* in the deep basin.

[39] We can also apply a one-box model to the deep BS water column below 2000 m to estimate the average sedimentary denitrification rate for the deep BS. Assuming a water residence time of 50 years, and using a depth-integrated nitrate deficit of 3.0 μmol L^{-1}, we calculate an average sedimentary denitrification rate of 230 μmol m^{-2} d^{-1} (Table 1). This calculation, unlike that for individual depth intervals below 2000 m, is not compromised by uncertainties in the details of the circulation in the lower 2000 m.

4.3.2. Rates Derived From Pore Water Measurements

[40] The pore water nitrate profiles clearly indicate that nitrate is being consumed by denitrification in the sediments (Figure 4). Are the pore water-derived denitrification rates high enough to produce the observed nitrate deficit in the water column? Nitrate fluxes into the sediments, on the basis of $[NO_3^-]$ profiles from the deep BS, range from 50 to 140 μmol N m^{-2} d^{-1}. Nitrate flux-based estimates of denitrification tend to underestimate the actual denitrification rate because they do not account for the coupling of nitrification and denitrification [*Christensen et al.*, 1987]. Given that, in most environments, nitrification-denitrification accounts for the major portion of total denitrification [e.g., *Christensen et al.*, 1987; *Middelburg et al.*, 1996; *Seitzinger*, 1988], we can expect the total denitrification rates in the BS to be much higher. We used the O_2 consumption rates calculated from electrode O_2 profiles to obtain estimates of the potential rate of nitrate production due to aerobic mineralization and nitrification [*Froelich et al.*, 1979] (Table 2). The latter were added to the diffusive flux of nitrate from the overlying water to yield rough estimates of total sedimentary denitrification rates (Table 2). The rates derived in this way are approximately 30% to 200% higher than the calculated net nitrate fluxes, so that denitrification rates in the BS basin likely range between 100 and 550 μmol N m^{-2} d^{-1} (Table 2). The pore water-derived estimates of nitrate flux and denitrification have large uncertainties. First, profile-based rates often underestimate the actual flux rates because of the uncertainty in core top concentration gradients and the potential for non-diffusive exchange [*Berelson et al.*, 1987; *Martin and Sayles*, 2004]. Second, the uncertain fate of reduced compounds (Mn, Fe, S) within the sediments imposes an additional source of error on O_2 flux-based nitrate production rates. Third, no matter how reliable the pore water-derived estimates of denitrification are, this rate can be extremely variable in marine sediments, at virtually every spatial scale. We cannot say which of the factors above is most important in the variability in our estimates for sedimentary denitrification rate. In any case, the pore water data do not make a

Table 2. Summary of Porewater Profile-Derived Fluxes and Regeneration Rates[a]

Core	Water Depth, m	Bottom Water [O_2], μmol L^{-1}	Nitrate Flux (Observed), μmol m^{-2} d^{-1}	Oxygen Flux (Observed), μmol m^{-2} d^{-1}	Aerobic N Remineralization (Estimated), μmol m^{-2} d^{-1}	Denitrification Rate (Estimated), μmol m^{-2} d^{-1}
			Northern BS Slope			
MC2	1105	38.3	−142	−1190	−138	−280
MC5	3349	96.4	−140 ± 45	−3580	−415	−555
			Bowers Ridge			
MC24[b]	714	22.7	−128 ± 6	−130	−15	−144
MC19[b]	855	20.4	−81 ± 4	−180	−21	−102
MC16	2216	68.5	−53 ± 1	−1090	−126	−179
MC29[b]	2850	92.2	40	−280	−32	0
MC31	2910	91.4	79	−740	−86	−7
			Southeastern BS Slope			
MC50[b]	1465	37.8	−117 ± 25	−180	−21	−138
MC56[b]	1015	30.3	−160	−280	−32	−192
MC43	1889	...	−79	−1200	−139	−218
MC47	1970	61.8	−112 ± 10	−340	−39	−151

[a]Nitrate fluxes represent means of duplicate determinations based on whole-core squeezing (WCS) and sample sectioning and centrifuging. For MC2, MC29, MC31, MC43, and MC56, only WCS yielded a high enough sample resolution to allow the determination of the linear concentration gradients in the upper 5 mm. Negative fluxes point into the sediments. Errors of nitrate fluxes represent standard deviations of duplicate flux determination. Errors for in situ micro electrode profiling-derived O_2 fluxes typically lie between ±10 and ±40% [*Reimers et al.*, 1986, 1992]. Instrumental precision is 1%.

[b]Core tops were contaminated with atmospheric O_2 and estimates on O_2 fluxes were calculated using the O_2 concentration difference between bottom water samples from Niskin bottle and points below 5 mm depth, where contamination was likely to be less important. Here estimates represent lower limits of actual O_2.

strong case for or against the validity of the amplitude of the N*-derived denitrification rate.

[41] However, the pore water data do provide mechanistic insight into the source of the deep nitrate deficit. The highest denitrification rate in the basin was observed at the deepest sampling location MC5 located at the foot of the especially steep slope of the northern BS continental margin, which is dissected by several canyons. We would normally expect lower denitrification rates at our deepest site because of reduced organic carbon rain at greater depth and higher bottom water O_2 concentrations. Two other cores at similar depth, MC29 and MC31, were raised from the bank of Bower's Ridge. In these cores, pore water derived denitrification rates were much lower than in shallower cores. Thus it appears that the geographic placement of MC5 is responsible for its high denitrification rate.

[42] We propose that MC5 is a critical indicator of the cause of the high basin-mean denitrification rate in the deep BS. We hypothesize that the combined high productivity of the Bering Shelf environment and the steepness of the BS continental slope cause large amounts of organic matter to be funneled to the base of the continental slope where it drives relatively high denitrification rates. Since the base of the steep slope is at ~3300–3500 m depth on average in the BS (Figure 5), this process may explain the fact that the N* minimum peaks in this depth range. A similar effect has been observed for the steep and highly dissected continental margin off the coast of California [*Jahnke et al.*, 1990; *Reimers et al.*, 1992].

4.4. The Deep Bering Sea: A Significant Sink of Fixed Nitrogen

[43] While the denitrification rates per sediment area reported in this study are roughly an order of magnitude lower than those measured in continental shelf sediments [e.g., *Devol*, 1991; *Hopkinson et al.*, 2001; *Lehmann et al.*, 2004], they are, at least in the deepest parts of the BS, as high as, or higher than, in other deep sea environments at equivalent water depths. Compared to our BS results, nitrate flux estimates from benthic chamber experiments on the deeper continental slope sediments off Central California are somewhat higher above 3000 m water depth (100–600 μmol m^{-2} d^{-1}), but significantly lower below 3000 m (10–120 μmol m^{-2} d^{-1}) [*Berelson et al.*, 1996]. On the basis of prognostic diagenetic model results, *Middelburg et al.* [1996] estimated global average denitrification rates for water depths between 2000 m and 4000 m of ~66 μmol m^{-2} d^{-1}, roughly an order of magnitude lower than those calculated for the deep BS slope sediments in MC5 and only 30% of the rate derived from water column N* (Figure 6).

[44] The total deep BS nitrate deficit amounts to 6.59×10^{13} g N. It is driven by sedimentary denitrification (over an area of 1080×10^3 km^2) at a loss rate of 1.27×10^{12} g N per year (based on the average model-based denitrification rate of 230 μmol m^{-2} d^{-1} for 2000–4000 m). This rate of nitrate consumption corresponds to about 50% of recent estimates of fixed N loss within BS shelf sediments [*Tanaka et al.*, 2004]. While the posited denitrification rates for the BS seem to be high for deep-sea sediments, they are consistent with the physical and biogeochemical characteristics of the deep BS. The nitrate deficit in the deep BS is a predictable result of sequestering basin waters for a moderate period of time in an environment that is generally conducive to sedimentary denitrification.

5. Summary and Concluding Remarks

[45] The combination of water column nutrient concentration and nitrate isotope data with in situ estimates of benthic nitrate flux provides new constraints on the nitrate

deficit in the deep BS. Neither $\delta^{15}N$ nor $\delta^{18}O$ show any increase in association with the nitrate deficit observed in the deep BS, indicating that sedimentary denitrification, which causes no net isotope fractionation of the residual bottom water nitrate, is the driver of nitrate loss in the BS.

[46] Water column nitrate integrates over large spatial and temporal scales and thus provides a robust measure of the mean basin-wide rate of sedimentary denitrification. On the basis of the distribution of N* in the water column and using an average water residence time of 50 years, we calculate that the average sedimentary denitrification below 2000 m water depth is 230 μmol m^{-2} d^{-1}. The sedimentary denitrification rate estimated from the distribution of N* is very sensitive to the rate of inflowing water from the SAP, particularly in the deepest portion of the basin, where the water volume is comparatively small. As a result, uncertainty in the rate of deep water exchange through the deep Kamchatka Strait will directly translate into uncertainty in denitrification rate. A more reliable picture of the circulation in the deep BS is needed to gain more confidence in calculated N*-based denitrification rate, especially its depth distribution.

[47] BS pore water profile-based estimates of sedimentary denitrification show relatively large variations, suggesting significant spatial heterogeneity in seafloor processes. While this clearly limits their utility for extrapolation to the entire deep BS, the in situ measurements offer insight into the conditions in the BS that lead to the generation of the deep nitrate deficit. In particular, the highest directly measured denitrification rate by far was observed in a multicore from the base of the slope along the northern boundary of the BS basin. This suggests that organic matter is efficiently funneled down the slope to its base, driving high abyssal denitrification rates. This interpretation is consistent with the unusual steepness of the NE continental slope in the BS. Combined with the facts that the BS is a nutrient-rich, highly productive environment and that the BS has relatively high deep water nitrate and low deep water O_2 concentrations, it is not difficult to imagine that denitrification rates in the deep BS are higher than elsewhere.

[48] However, the deep nitrate deficit in the BS does not appear to result solely from high area-normalized rates of benthic denitrification. Much of the seafloor area is between 3 and 4 km, so that even a comparatively low denitrification rate would lead to maximal nitrate loss from these depths, as observed. Parameters in favor of high area-normalized denitrification rates in deep sediments and a flat seafloor in the basin converge to allow for the accumulation of the observed deep Bering basin nitrate deficit.

[49] Low N* in the lower latitude Pacific is not restricted to the regions and depths of water column suboxia [*Deutsch et al.*, 2001; *Gruber and Sarmiento*, 1997]. Some of these low-N* regions clearly reflect the outward transport of a denitrification (i.e., negative N*) signal from the suboxic zones [*Sigman et al.*, 2003]. However, some of these O_2-bearing regions of low N* may be driven by sedimentary denitrification, a possibility that our BS study highlights. Isotopic studies of these regions should be able to distinguish between these explanations. Recent studies argue for the dominance of benthic denitrification in the global N budget [*Brandes and Devol*, 2002; *Codispoti et al.*, 2001; *Middelburg et al.*, 1996], and some of them [*Middelburg et al.*, 1996] conclude that global denitrification occurring in continental slope and deep-sea sediments by far exceeds denitrification in shelf areas. Coupling of nutrient ratio data with nitrate N and O isotope measurements may allow us to test these assertions and identify the regions most responsible for nitrate loss.

[50] **Acknowledgments.** We thank L. Keigwin, N. Driscoll, and J. Brigham-Grette for their invitation to take part in the BS cruise, and L. Codispoti for onboard nutrient analyses. We also thank R. Ho for technical assistance. This study was supported by NSF grants OCE-0136449 and OCE-9981479 to D. M. S., OCE-0118126 and OCE-0324987 to D. C. M., and DFG grant LE 1326/1-1 to M. F. L. The BS cruise was funded by grant OPP-9912122.

References

Alldredge, A., and Y. Cohen (1987), Can microscale chemical patches persist in the sea? Microelectrode study of marine snow, fecal pellets, *Science*, *235*, 687–691.

Altabet, M. A. (2001), Nitrogen isotopic evidence for micronutrient control of fractional NO_3-utilization in the equatorial Pacific, *Limnol. Oceanogr.*, *46*, 368–380.

Altabet, M. A., and R. Francois (1994), Sedimentary nitrogen isotopic ratio as a recorder for surface ocean nitrate utilization, *Global Biogeochem. Cycles*, *8*(1), 103–116.

Altabet, M. A., et al. (1999), The nitrogen isotope biogeochemistry of sinking particles from the margin of the Eastern North Pacific, *Deep Sea Res., Part I*, *46*, 655–679.

Barford, C. C., J. P. Montoya, M. A. Altabet, and R. Mitchell (1999), Steady-state nitrogen effects of N_2 and N_2O production in *Paraoccus denitrificans*, *Appl. Environ. Microbiol.*, *65*(3), 989–994.

Bender, M. L. (1990), The $\delta^{18}O$ of dissolved O_2 in seawater: A unique tracer of circulation and respiration in the deep sea, *J. Geophys. Res.*, *95*(C12), 22,243–22,252.

Berelson, W. M., D. E. Hammond, and K. S. Johnson (1987), Benthic fluxes and the cycling of biogenic silica and carbon in two southern California borderland basins, *Geochim. Cosmochim. Acta*, *51*(6), 1345–1363.

Berelson, W. M., et al. (1996), Biogenic matter diagenesis on the sea floor: A comparison between two continental margin transects, *J. Mar. Res.*, *54*(4), 731–762.

Bohlke, J. K., S. J. Mroczkowski, and T. B. Coplen (2003), Oxygen isotopes in nitrate: New reference materials for O-18:O-17:O-16 measurements and observations on nitrate-water equilibration, *Rapid Commun. Mass Spectrom.*, *17*(16), 1835–1846.

Boudreau, B. P. (1997), *Diagenetic Models and Their Implementation*, 417 pp., Springer, New York.

Braman, R. S., and S. A. Hendrix (1989), Nanogram nitrite and nitrate determination in environmental and biological-materials by vanadium (III) reduction with chemi-luminescence detection, *Anal. Chem.*, *61*, 2715–2718.

Brandes, J. A., and A. H. Devol (1995), Simultaneous nitrate and oxygen respiration in coastal sediments—Evidence for discrete diagenesis, *J. Mar. Res.*, *53*(5), 771–797.

Brandes, J. A., and A. H. Devol (1997), Isotopic fractionation of oxygen and nitrogen in coastal marine sediments, *Geochim. Cosmochim. Acta*, *61*(9), 1793–1801.

Brandes, J. A., and A. H. Devol (2002), A global marine-fixed nitrogen isotopic budget: Implications for Holocene nitrogen cycling, *Global Biogeochem. Cycles*, *16*(4), 1120, doi:10.1029/2001GB001856.

Brandes, J. A., A. H. Devol, T. Yoshinari, D. A. Jayakumar, and S. W. A. Naqvi (1998), Isotopic composition of nitrate in the central Arabian Sea and eastern tropical North Pacific: A tracer for mixing and nitrogen cycles, *Limnol. Oceanogr.*, *43*, 1680–1689.

Broecker, W. S., and T.-H. Peng (1982), *Tracers in the Sea*, Lamont-Doherty Geol. Obs., Palisades, New York.

Casciotti, K. L., D. M. Sigman, M. G. Hastings, J. K. Bohlke, and A. Hilkert (2002), Measurement of the oxygen isotopic composition of nitrate in seawater and freshwater using the denitrifier method, *Anal. Chem.*, *74*, 4905–4912.

Christensen, J., J. Murray, A. Devol, and L. Codispoti (1987), Denitrification in continental shelf sediments has major impact on the ocean nitrogen budget, *Global Biogeochem. Cycles*, *1*(2), 97–116.

Cline, J. D., and I. R. Kaplan (1975), Isotopic fractionation of dissolved nitrate during denitrification in the eastern tropical North Pacific Ocean, *Mar. Chem.*, *3*(4), 271–299.

Coachman, L., T. Whitledge, and J. Goehring (1999), Silica in Bering Sea deep and bottom water, in *Dynamics of the Bering Sea*, edited by T. Loughlin and K. Ohtani, pp. 285–309, Univ. of Alaska Sea Grant, Fairbanks.

Codispoti, L. A., et al. (2001), The oceanic fixed nitrogen and nitrous oxide budgets: Moving targets as we enter the anthropocene?, *Sci. Mar.*, *65*, 85–105.

Codispoti, L. A., T. Yoshinari, and A. H. Devol (2005), Suboxic respiration in the oceanic water column, in *Respiration in Aquatic Ecosystems*, edited by P. A. delGiorgio and P. B. Williams, 225–247, Blackwell Sci., Malden, Mass.

Deutsch, C., N. Gruber, R. M. Key, J. L. Sarmiento, and A. Ganachaud (2001), Denitrification and N-2 fixation in the Pacific Ocean, *Global Biogeochem. Cycles*, *15*(2), 483–506.

Deutsch, C., D. M. Sigman, R. C. Thunell, A. N. Meckler, and G. H. Haug (2004), Isotopic constraints on glacial/interglacial changes in the oceanic nitrogen budget, *Global Biogeochem. Cycles*, *18*, GB4012, doi:10.1029/2003GB002189.

Devol, A. H. (1991), Direct measurement of nitrogen gas fluxes from continental-shelf sediments, *Nature*, *349*, 319–321.

Devol, A. H., L. A. Codispoti, and J. P. Christensen (1997), Summer and winter denitrification rates in western Arctic shelf sediments, *Cont. Shelf Res.*, *17*(9), 1029–1050.

Froelich, P. N., et al. (1979), Early Oxidation of organic-matter in pelagic sediments of the eastern equatorial Atlantic—Suboxic diagenesis, *Geochim. Cosmochim. Acta*, *43*(7), 1075–1090.

Gonfiantini, R., W. Stichler, and K. Rozanski (1995), Standards and intercomparison materials distributed by the International Atomic Energy Agency for stable isotope measurements, *IAEA-TECDOC-825*, Int. At. Energy Agency, Vienna.

Granger, J., D. M. Sigman, J. A. Needoba, and P. J. Harrison (2004), Coupled nitrogen and oxygen isotope fractionation of nitrate during assimilation by cultures of marine phytoplankton, *Limnol. Oceanogr.*, *49*, 1763–1773.

Gruber, N., and J. L. Sarmiento (1997), Global patterns of marine nitrogen fixation and denitrification, *Global Biogeochem. Cycles*, *11*(2), 235–266.

Hopkinson, C. S., A. E. Giblin, and J. Tucker (2001), Benthic metabolism and nutrient regeneration on the continental shelf of eastern Massachusetts, USA, *Mar. Ecol. Prog. Ser.*, *224*, 1–19.

Ingall, E., and R. Jahnke (1994), Evidence for enhanced phosphorus regeneration from marine-sediments overlain by oxygen depleted waters, *Geochim. Cosmochim. Acta*, *58*(11), 2571–2575.

Jahnke, R. A., C. E. Reimers, and D. B. Craven (1990), Intensification of recycling of organic matter at the sea floor near ocean margins, *Nature*, *348*, 50–54.

Koike, I., and A. Hattori (1979), Estimates of denitrification in sediments of the Bering Sea shelf, *Deep Sea Res., Part A*, *26*, 409–415.

Kuypers, M. M. M., A. O. Sliekers, G. Lavik, M. Schmid, B. B. Jørgensen, J. G. Kuenen, J. S. Sinninghe Damsté, M. Strous, and M. S. M. Jetten (2003), Anaerobic ammonium oxidation by anammox bacteria in the Black Sea, *Nature*, *422*, 608–611.

Lehmann, M. F., D. M. Sigman, D. C. McCorkle, W. M. Berelson, B. Brunelle, and S. S. Hoffmann (2002), The nitrogen and oxygen isotope composition of porewater nitrate from Bering Sea sediments, *Eos Trans. AGU*, *83*(47), Fall Meet. Suppl., Abstract PP51A-0297.

Lehmann, M. F., P. Reichert, S. M. Bernasconi, A. Barbieri, and J. A. McKenzie (2003), Modelling nitrogen and oxygen isotope fractionation during denitrification in a lacustrine redox-transition zone, *Geochim. Cosmochim. Acta*, *67*(14), 2529–2542.

Lehmann, M. F., D. M. Sigman, and W. M. Berelson (2004), Coupling the $^{15}N/^{14}N$ and $^{18}O/^{16}O$ of nitrate as a constraint on benthic nitrogen cycling, *Mar. Chem.*, *88*(1–2), 1–20.

Liu, K. K., and I. R. Kaplan (1989), The eastern tropical Pacific as a source of ^{15}N-enriched nitrate in seawater off southern California, *Limnol. Oceanogr.*, *34*, 820–830.

Lloyd, D. (1993), Aerobic denitrification in soils and sediments—From fallacies to facts, *Trends Ecol. Evol.*, *8*(10), 352–356.

Logan, B. E., and A. L. Alldredge (1989), Potential for increased nutrient-uptake by flocculating diatoms, *Mar. Biol.*, *101*(4), 443–450.

Mariotti, A., et al. (1981), Experimental determination of nitrogen kinetic isotope fractionation: Some principles; illustration for the denitrification and nitrification processes, *Plant Soil*, *62*, 413–430.

Martin, W. R., and F. L. Sayles (2004), Organic matter cycling in sediments of the continental margin in the northwest Atlantic Ocean, *Deep Sea Res., Part I*, *51*, 457–489.

Martin, W. R., M. Bender, M. Leinen, and J. Orchardo (1991), Benthic organic-carbon degradation and biogenic silica dissolution in the central equatorial Pacific, *Deep Sea Res., Part A*, *38*, 1481–1516.

Middelburg, J. J., K. Soetaert, P. M. J. Herman, and C. H. R. Heip (1996), Denitrification in marine sediments: A model study, *Global Biogeochem. Cycles*, *10*(4), 661–673.

Ploug, H. (2001), Small-scale oxygen fluxes and remineralization in sinking aggregates, *Limnol. Oceanogr.*, *46*, 1624–1631.

Ploug, H., S. Hietanen, and J. Kuparinen (2002), Diffusion and advection within and around sinking, porous diatom aggregates, *Limnol. Oceanogr.*, *47*, 1129–1136.

Reed, R. K., G. V. Khen, P. J. Stabeno, and A. V. Verkhunov (1993), Water properties and flow over the deep Bering Sea Basin, summer 1991, *Deep Sea Res., Part A*, *40*, 2325–2334.

Reimers, C. E., K. M. Fischer, R. Merewether, K. L. Smith, and R. A. Jahnke (1986), Oxygen microprofiles measured in situ in deep ocean sediments, *Nature*, *320*, 741–744.

Reimers, C. E., R. A. Jahnke, and D. C. McCorkle (1992), Carbon fluxes and burial rates over the continental slope and rise off central California with implications for the global carbon cycle, *Global Biogeochem. Cycles*, *6*(2), 199–224.

Revesz, K., J. K. Böhlke, and T. Yoshinari (1997), Determination of $\delta^{18}O$ and $\delta^{15}N$ in nitrate, *Anal. Chem.*, *69*, 4375–4380.

Saino, T., K. Myata, and A. Hattori (1979), Primary productivity in the Bering and Chukchi seas and in the northern North Pacific in 1978 summer, *Bull. Plankton Soc. Jpn.*, *26*, 96–103.

Scientific Committee on Oceanographic Research (SCOR) (1996), Protocols for the Joint Global Ocean Flux Study (JGOFS) core measurements, *JGOFS Rep. 19*, Paris.

Seitzinger, S. P. (1988), Denitrification in freshwater and coastal marine ecosystems: Ecological and geochemical significance, *Limnol. Oceanogr.*, *33*, 702–724.

Sigman, D. M., et al. (2001), A bacterial method for the nitrogen isotopic analysis of nitrate in seawater and freshwater, *Anal. Chem.*, *73*, 4145–4153.

Sigman, D. M., et al. (2003), Distinguishing between water column and sedimentary denitrification in the Santa Barbara Basin using the nitrogen isotopes of nitrate, *Geochem. Geophys. Geosyst.*, *4*(5), 1040, doi:10.1029/2002GC000384.

Sigman, D. M., J. Granger, P. DiFiore, M. Lehmann, R. Ho, G. Cane, and A. van Geen (2005), Coupled nitrogen and oxygen isotope measurements of nitrate along the eastern North Pacific margin, *Global Biogeochem. Cycles*, doi:10.1029/2005GB002458, in press.

Silva, S. R., et al. (2000), A new method for collection of nitrate from fresh water and the analysis of nitrogen and oxygen isotope ratios, *J. Hydrol.*, *228*, 22–36.

Tanaka, T., et al. (2004), N deficiency in a well-oxygenated cold bottom water over the Bering Sea shelf: Influence of sedimentary denitrification, *Cont. Shelf Res.*, *24*(12), 1271–1283.

Toggweiler, J. (1983), I) A multi-tracer study of the abyssal water column of the deep Bering Sea, including sediment interactions; II) A six zone regionalized model for bomb radiotracers and CO_2 in the upper kilometer of the Pacific Ocean, Ph.D. thesis, 425 pp., Columbia Univ., New York.

Tsunogai, S., M. Kusakabe, H. Lizumi, and A. Hattori (1979), Hydrographic features of the deep water of the Bering Sea: The sea of silica, *Deep Sea Res., Part A*, *26*, 641–659.

Voss, M., J. W. Dippner, and J. P. Montoya (2001), Nitrogen isotope patterns in the oxygen-deficient waters of the eastern tropical North Pacific Ocean, *Deep Sea Res., Part I*, *48*, 1905–1921.

Wada, E., and A. Hattori (1978), Nitrogen isotope effects in the assimilation of inorganic nitrogenous compounds by marine diatoms, *Geomicrobiol. J.*, *1*, 85–101.

Warner, M. J., and G. I. Roden (1995), Chlorofluorocarbon evidence for recent ventilation of the Deep Bering Sea, *Nature*, *373*, 409–412.

Waser, N. A. D., P. J. Harrison, B. Nielsen, S. E. Calvert, and D. H. Turpin (1998), Nitrogen isotope fractionation during the uptake and assimilation of nitrate, nitrite, ammonium, and urea by a marine diatom, *Limnol. Oceanogr.*, *43*, 215–224.

Whitledge, T. E., S. C. Malloy, C. J. Patton, and C. D. Wirick (1981), Automated nutrient analysis in seawater, *Tech. Rep. BNL-51398*, Brookhaven Natl. Lab., Upton, N. Y.

Wolgast, D. M., A. F. Carlucci, and J. E. Bauer (1998), Nitrate respiration associated with detrital aggregates in aerobic bottom waters of the abyssal NE Pacific, *Deep Sea Res., Part II*, *45*, 881–892.

Yoshinari, T., and I. Koike (1994), The use of stable isotopes for the study of gaseous nitrogen species in marine environments, in *Stable Isotopes in Ecology and Environmental Science*, edited by K. Lajtha and R. Michener, pp. 114–137, Blackwell Sci., Norwell, Mass.

B. G. Brunelle, G. Cane, and D. M. Sigman, Department of Geosciences, Princeton University, Guyot Hall, Princeton, NJ 08544, USA.

J. Clement, Naval Postgraduate School, Dept. of Oceanography, Monterey, CA 93943, USA.

S. Hoffmann, and D. C. McCorkle, Woods Hole Oceanographic Institution, Woods Hole, MA 02543, USA.

M. F. Lehmann, Geochemistry and Geodynamics Research Center (GEOTOP-UQAM-McGill), University of Quebec at Montreal, Montreal, Quebec, H3C 3P8, Canada. (lehmann.moritz@uqam.ca)

M. Kienast, Department of Oceanography, Dalhousie University, Halifax, Nova Scotia, B3H 4J1, Canada.

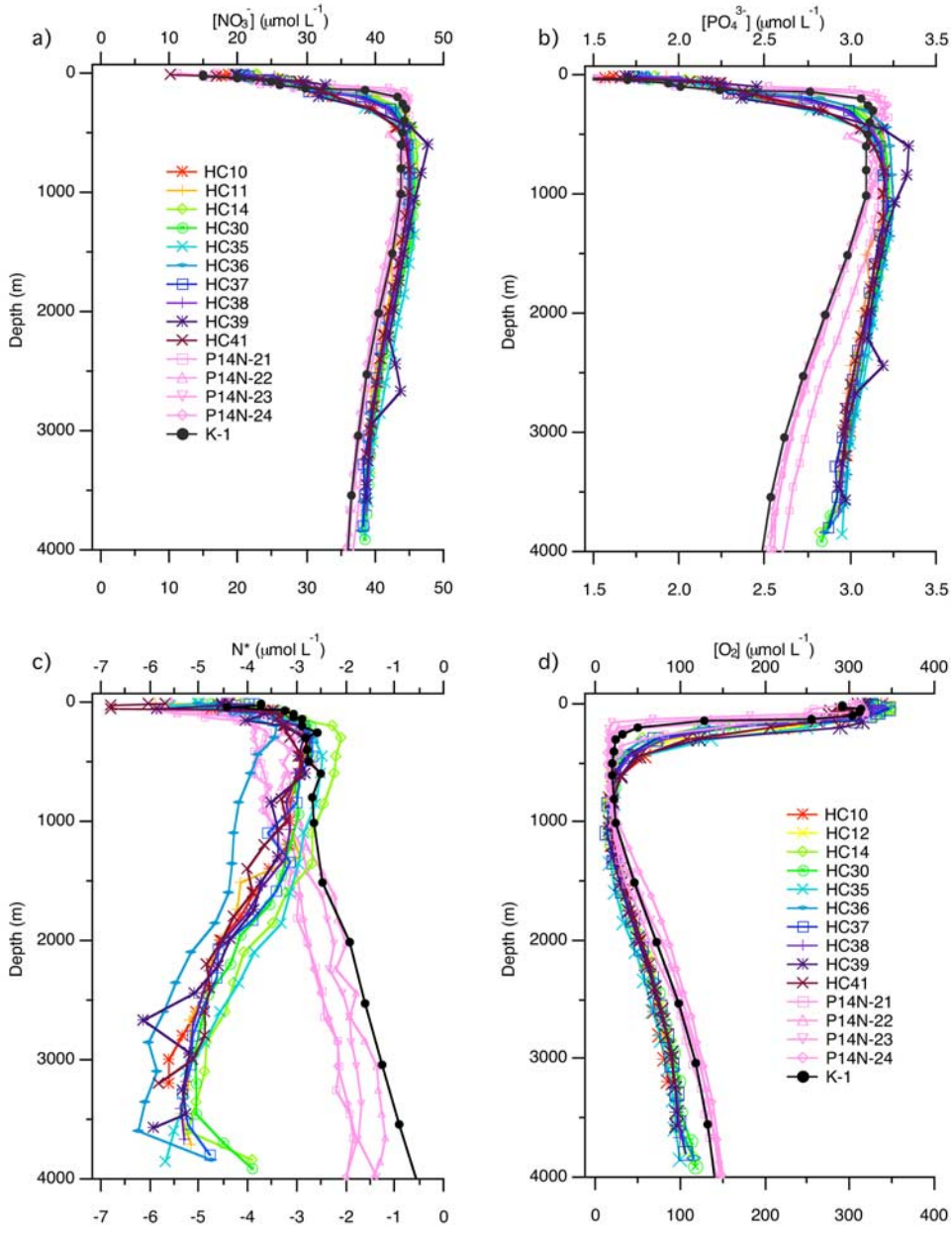

Figure 2. Water column profiles of (a) $[NO_3^-]$, (b) $[PO_4^{3-}]$, (c) N*, and (d) $[O_2]$ for Bering Sea stations (HC) and Stations from the subarctic Pacific (P14N and K1). Nutrient data are not available for BS station HC12, and $[O_2]$ data are not available for BS station HC11. Note the stoichiometric differences between the BS and the SAP.

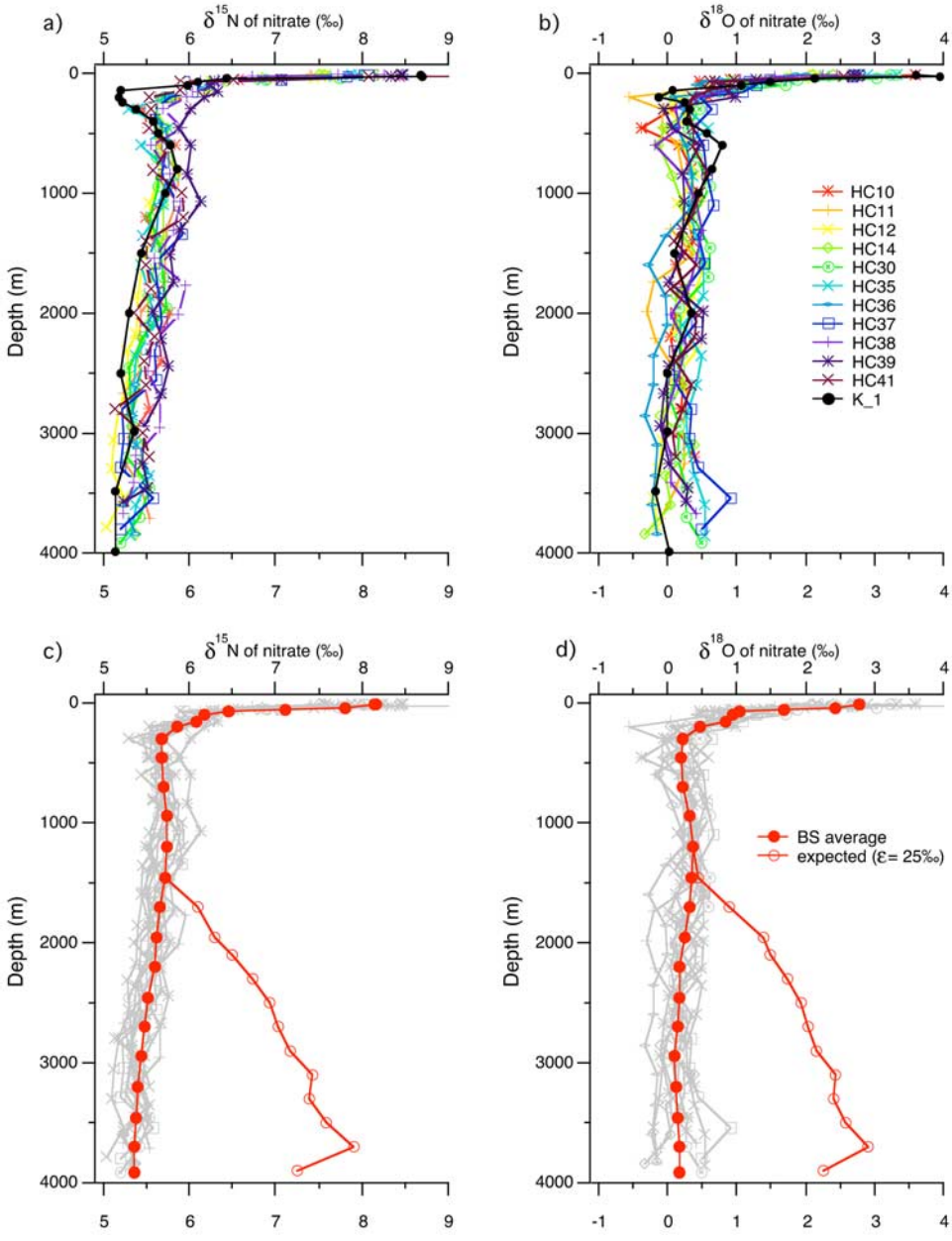

Figure 3. Water column profiles of (a) nitrate $\delta^{15}N$ and (b) nitrate $\delta^{18}O$ for Bering Sea stations (HC) and Station K1 from the subarctic Pacific (K1 nitrate isotope data are taken from M. Kienast et al. (manuscript in preparation, 2005)). (c, d) Solid circles represent depth-binned average nitrate isotope values for all the BS hydrocasts superimposed on the profiles shown in Figures 3a and 3b. Expected N and O isotope ratios (open symbols in Figures 3c and 3d) are based on an assumed isotope effects $\varepsilon_{15} = \varepsilon_{18} = 25‰$ for denitrification and the observed nitrate deficit below 1500 m water depth, assuming a steady state balance between gross supply of SAP nitrate, partial nitrate consumption, and export by circulation of the remaining nitrate.

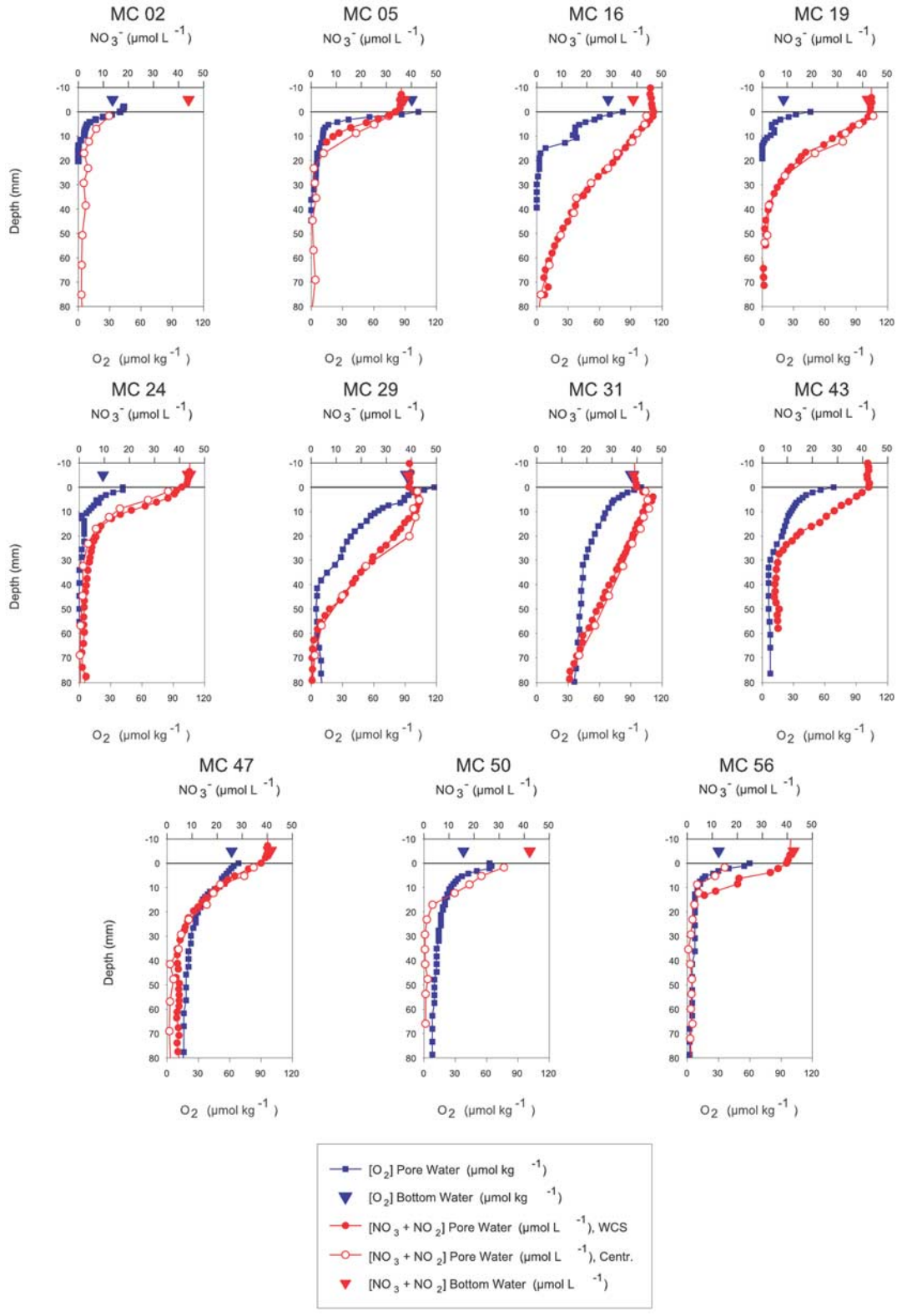

Figure 4. Pore water profiles ($[NO_3^- + NO_2^-]$ and $[O_2]$) for multicores from the Bering Basin. O_2 profiles were generated using a shipboard minielectrode profiler. Deviations between the Winkler-derived $[O_2]$ in the bottom water (sample taken from Niskin bottle) (open triangle) and electrode-derived $[O_2]$ at the sediment water interface are due to atmospheric contamination during shipboard profiling. Low non-zero $[O_2]$ values deep in some profiles may reflect bottom water leakage along the electrode, rather than real pore water $[O_2]$.

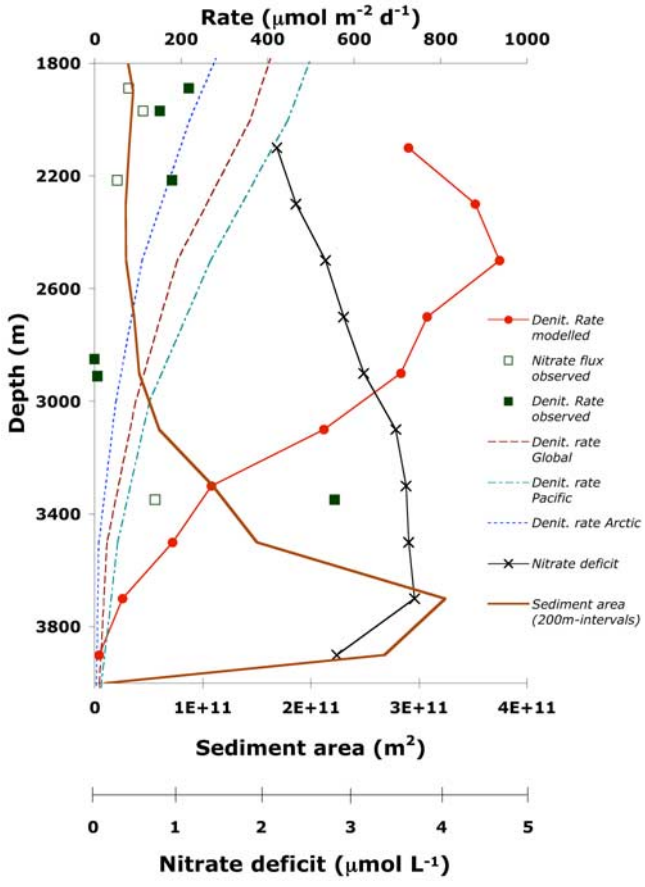

Figure 6. Compilation of directly determined nitrate fluxes and sedimentary denitrification rates (below 1900 m), and indirectly determined mean sedimentary denitrification rates based on the distribution of N*, compared to estimated sedimentary denitrification rates as a function of depth for the global ocean, the Pacific Ocean, and the Arctic Ocean from *Middelburg et al.* [1996]. Also plotted are the seafloor sediment area for given water depths (200-m intervals), and the apparent nitrate deficit calculated from the N* difference between the BS and the SAP. Apparent nitrate fluxes out of the sediments of MC29 and MC31 are not shown.

View publication stats